Journal of Simulation and Analysis of Novel Technologies in Mechanical Engineering
15 (2) (2023) 0063~0077

Research article

Effect of wind speed on the drag force and wall shear stress of domes in historical mosques of Iran: a case study

Iman Pishkar[1, *], Mehdi Jahangiri[b], Rouhollah Yadollahi Farsani[b], Ayoub Khosravi Farsani[c]

[1]*Department of Mechanical engineering, Payame Noor University (PNU), P.O. Box 19395-4697, Tehran, Iran.*
[2]*Energy Research Center, Shahrekord Branch, Islamic Azad University, Shahrekord, Iran.*
[3]*Department of Mechanical Engineering, Faculty of Boroujen, Technical and Vocational University (TVU), Chaharmahal and Bakhtiari, Iran.*

[*] e.pishkar@pnu.ac.ir

(Manuscript Received --- 27 Jan. 2023; Revised --- 10 May 2023; Accepted --- 30 May 2023)

Abstract

Climatic conditions have a great impact on the erosion of the coverage and the materials destruction of the dome gradually. Therefore, studying the shape and form of the dome in historic mosques can greatly assist to identify the affected points of the different types of the domes and provide solutions to prevent early destruction of the domes. In the present work, the turbulent flow of wind around the four samples of different domes is investigated, using ANSYS CFX software, to determine which parts of the dome geometry are most affected by wind and erosion. In the present work, for the first time, it will be tried to study different types of domes used in different climates and their geometric shapes, besides conducting research to prevent early erosion. The results demonstrated that a large vortex has shaped on the opposite side of the wind, which affects the area behind the dome and causes a negative pressure through velocity reduction. Also, the highest wind velocity is formed a little higher and hinder of the dome. The results of the shear stress on the crown of the dome for the four cases illustrated that for the dome type W4, the highest shear stress is about 15 Pa on the face against the wind and it is about 12 Pa for that of W1 on the face opposite the wind. It should be noted that the position of the most stresses on the dome crown corresponding to the most damage to the building is estimated.

Keywords: Dome geometry, Climatic factors, Historical mosques, Shear stress, CFD.

Nomenclature

Cij	Model constant, -
D	Diameter, m
F	Drag force, N
G	Generation of turbulence kinetic energy
g	Gravity, 9.81 $m.s^{-2}$
k	Turbulent kinetic energy, m^2/s^2
p	Pressure, N/m^2
Re	Reynolds number, -

Greek Symbols

ε	Dissipation rate,m^2/s^3
μ	Dynamic viscosity , $N\ s/m^2$
τ	Shear stress, m^2/s
ρ	Density, kg/m^3
σ	Turbulent Prandtl numbers, -
ν	Cinematic viscosity, Pa.s

Subscripts			
S	Source term, -	i,j,k	Spatial indices, -
u, v	Velocity, m/s	ε	ε-equatiom, -
Y_M	Contribution of the fluctuating dilatation in compressible turbulence to the overall dissipation rate, -	K	k-equation, -
CFD	Computational fluid dynamic, -	t	Turbulence, -
C_p	Pressure coefficient, -	k	kinematic
RANS	Reynolds-Averaged Navier-Stokes, -		

1- Introduction

The dome, one of the most important structural elements, was utilized by the Iranians due to its capability to cover a large area more than any other type of covering [1, 2]. Domes in Iran during the Sassanid era (224-651 AD) were transferred to the peak of Iranian architecture and they gradually developed in different periods until the Safavid era (1732-1501) when the last generation of Iranian domes with distinguished features and amazing tiles were identified [3]. Among the oldest Iranian domes, we can mention the Persian girl castle [4, 5], Firoozabad fire temple [6] and Niasar fire temple [7], which are remained from the Parthian and Samani eras. The Iranian domes are created with the combination of several arcs and their rotations around the axis of symmetry [8]. Their stability is higher than the European ones, which are generally built from the rotation of a quarter circle [9, 10].

Some researchers consider the generation causes and the most important feature of the geometric shape of the dome to be the human scale under the dome and the creation of proportions between the external components and the dome [11]. Over time, the architectural compositions of the Iranian domes have undergone fundamental changes in terms of structure and aesthetic. Since they appeared in different dynasties, especially in Islamic periods, and finally concluded with the emergence of three main types of domes: conical, pointed and bulbous [12]. However, in Iran, over time, the construction of conical and polygonal domes changed into an obsolete tradition [13]. According to another classification, the domes can be categorized into six groups in terms of form and construction method; including single-shelled eggy domes, continuous double-shelled domes, racked domes with the rib vaults, discontinuous rock domes, discontinuous domes covered with the exterior Nar covering and three-layered domes [14].

The dome has been applied in post-Islamic architecture in many buildings, especially religious ones, including mosques [15-17]. Therefore, its study based on climatic factors is of high importance. On the other hand, weather condition and type of climate have always been an issue that human has coped with over thousand years of experience. Undoubtedly, many difficulties for people living in hot dry and hot humid climates, such as scorching sun, high heat and temperature difference and its fluctuations over the day and its reduction to a considerable extent in the night breeze have been considered. Hard summers and cold winters caused by desert climate and in some cases, dust storms as

well as dry, hot and unpleasant winds have made people to find a way.

Followed that, the recent laboratory studies and simulations in the field of domes in Iran and the world will be reviewed.

Faghih and Bahadori (2009) experimentally evaluated the wind pressure coefficient (C_P) on a domed roof. This experiment was done in a wind tunnel with a maximum speed of 70 m/s on a dome model at a scale of 1/10. Twelve openings were located in the dome collar and one at its apex. The experiment focused on the dome CP in three different modes. The results revealed that the CP at the dome collar has reached its maximum, when all the openings and holes were opened or closed, and the least CP was measured at the apex when the openings and holes were closed [18].

Cheng and Fu (2010) carried out a series of wind tunnel experiments to investigate the effects of the Reynolds number on the aerodynamic features of the hemispherical dome over the smooth and turbulent boundary layer flow. The results illustrated that in the smooth flow, the distribution of the wind pressure became relatively stable after $Re > 3.0 \times 10^5$. While in the turbulent flow, the pressure becomes independent of the Reynolds number [19].

Faghih and Bahadori (2011) studied analytically how domed roofs, regarding various parameters such as airflow around them, solar radiation, transition of radiant heat through the sky and earth as well as apertures available in a religious school in Yazd, can meet the thermal needs in hot seasons. The results indicated that the domed roof provides better thermal comfort in summer compared to the flat roof. In addition, the openings led to passive airflow inside the building, which was useful to provide thermal comfort [20].

Abohela *et al.* (2013) investigated the effect of wind flow around six different roof shapes (flat, domed, gabled, pyramidal, vaulted and wedged) to cover an insulated cubic building with 6 m high, to determining the optimal height and roof shape to install a wind turbine with the use CFD. The effect of roof shapes regarding to the patterns of wind flow, turbulence intensity and flow velocity was examined. According to the study, the best place to install the wind turbine was above the domed roof, 1.3 times the height of the building, where the maximum streamwise wind velocity was achieved, being higher than the flow velocity in the same place without the building in flow field [21].

Sun et al. (2013) investigated the characteristics of the wind pressure spectrum on spherical domes based on a series of wind tunnel experiments. The results indicate that rise/span ratio shows more significant influence on the spectral shape and amplitude in a high frequency range $fD/U > 1.0$ than the height/span ratio [22].

Mahdavinejad *et al.* (2014) employed mathematical analysis and CFD to determine the performance of a flat and domed roof in terms of airflow and internal temperature in climate of Tehran. The results illustrated that the domed roof resulted a reduction in the indoor air temperature by 8 K compared to the flat roof. Also the geometry of the domed roof causes higher pressure difference between the two sides of the wind and the two sides of the house in comparison with the flat roof house, resulting in better natural airflow. Furthermore, gain and heat loss were less with a domed roof compared to a flat roof [23].

Soleimani *et al.* (2016) calculated computational modeling of ventilation derived from wind and buoyancy in a geodesic dome building in hot climate. The Reynolds-Averaged Navier-Stokes (RANS) three-dimensional equations were solved using the CFD ANSYS FLUENT software. The results represented that the use of overhead roof openings as a natural ventilation strategy in winter is beneficial and can both reduce the indoor temperature and bring in fresh air. Also, natural ventilation using roof openings cannot meet the cooling needs over hot summer and complementary cooling solutions should be considered [24].

Zhou *et al.* (2017) investigated the effects of geometric parameters of roofs and land type on wind pressure distribution based on data obtained from wind tunnel tests. Then, the wind loads of the full-scale structures were predicted by CFD, and the effectiveness of the numerical results was further verified by existing wind tunnel tests on space structures. Finally, the effects of aspect ratios, especially height-to-span ratio, height-to-span ratio, length-to-span ratio, etc., and terrain type on the wind pressure field of typical spatial structures were presented by comparative analyzes of roof wind pressure distribution investigated by CFD [25].

Khosrowjerdi et al (2021) in a study investigated the effect of wind load on traditional dome buildings using CFD techniques. In this research, fifteen common Iranian dome architectures with composite arches were selected to numerically investigate the changes in wind pressure coefficient (C_p) on these domes at different heights and angles. This study showed that the shape of the dome has a significant effect on the amount of wind load on it. So that the amount of C_p in a certain height range in different domes can have a significant difference [26].

Khosrowjerdi and Sarkardeh (2022) investigated the effect of wind load on double-arched domes with different arch heights. The results indicated the effect of different variables of the height of the arches, failure at the junction of two arches and the surface of the connection of two arches on the C_p parameter [27].

Nejati *et al* (2023) investigated the effect of wind on scallop domes using CFD and wind tunnel tests. Analyzes were performed through ANSYS Fluent software. The results showed that the wind pressure on scallop domes is significantly different from the wind pressure on spherical domes [28].

The analysis of the dome as one of the main components of religious places should be investigated according to climatic factors and erosion. Also, by providing some solutions, a step should be taken to conserve it. Also the present work will examine the different types of domes in several climates, the effect of wind speed and pressure on various parts of the dome. The present work consists of diverse samples of different domes, but does not consider all the shells of the dome and will only investigate the effect of wind speed on the outer shell of the Iranian ones. As shown in the recent studies, wind flow affects significantly the structure and performance of the domed roofs, and certainly it can have tangible effects on the dome structure in a long time. Therefore, in the present work, for the first time, it will be tried to study different types of domes used in different climates and their geometric shapes, besides conducting research to prevent early erosion.

According to the above, in the present work, effective parameters have been

investigated using the k-ε turbulence model in ANSYS CFX software. The contours of pressure, wind speed and drag force were investigated and the shear stress diagram of the wall along the arc of the dome was also evaluated.

2- Present work

The various forms of domes, simulated in the software, are shown in Fig. 1. As it is obvious, the four different forms are named W1 to W4 from left to right respectively. It should be noted that since only the effect of the dome arch on the analysis of the passing wind flow has been considered, in the simulations, the vertical wall of the domes has been omitted in order to reduce the computational time.

To investigate the influences of wind flow on the geometric shapes of different domes, it is essential to model the wind flow on the dome using ANSYS CFX fluid flow modeling software. To be able to compare the results of different domes with each other, the best solution is to apply the method of dimensional analysis. In this method, the definition of the Reynolds dimensionless number is used to investigate the effects of airflow on solid objects [29, 30]. This number is the ratio of dynamic forces to viscous forces. By obtaining the results for a constant Reynolds number, the outcomes can be used for different conditions by changing the dimensions or boundary conditions.

3- Governing equations

The governing equations of the wind flow around the dome including the continuity equation [31], the momentum equation [32], the k equation [33], and the ε equation [34], in the steady state condition, are given in equations 1 to 4, respectively. The parameters used in the software are described in references [35, 36] and due to summarizing are not presented. One reason that the air flow is assumed to be turbulent is since that any obstruction against the flow of the fluid causes turbulence currents and the formation of vortices behind the domes [37, 38].

$$\nabla.(\rho\vec{v}) = S_m \tag{1}$$

$$\nabla.(\rho\vec{v}\vec{v}) = -\nabla p + \nabla.(\bar{\bar{\tau}}) + \rho\vec{g} + \vec{F} \tag{2}$$

$$\frac{\partial}{\partial x_i}(\rho k u_i) = \frac{\partial}{\partial x_j}\left[\left(\mu + \frac{\mu_t}{\sigma_k}\right)\frac{\partial k}{\partial x_j}\right] + G_k + G_b - \rho\varepsilon - Y_M + S_k \tag{3}$$

$$\frac{\partial}{\partial x_i}(\rho\varepsilon u_i) = \frac{\partial}{\partial x_j}\left[\left(\mu + \frac{\mu_t}{\sigma_\varepsilon}\right)\frac{\partial \varepsilon}{\partial x_j}\right] + C_{1\varepsilon}\frac{\varepsilon}{k}(G_k + C_{3\varepsilon}G_b) - C_{2\varepsilon}\rho\frac{\varepsilon^2}{k} + S_\varepsilon \tag{4}$$

4- Boundary conditions

Fig. 2 illustrates a view of the performed grids on solution domains which the dome W1 has been presented as an example. As can be seen on Fig. 2, regarding that in solving the governing questions, the force and stress on the dome are considered for calculation, so near the surface of the dome where the velocity gradients is too high due to air and wall interaction, the grid has been refined for solving the domain more perciesly.

To reduce the cost of computing time at further distances of the dome, the grid has become coarser [39]. It should be noted that the number of computational cells is

selected in such a way that the resolvent is converged and the convergence criterion is that the drag coefficient parameter is not changed. For meshing, due to the presence of curvature and sharp edges in the studied geometries, unstructured (triangular) mesh has been used.

The assumed boundary conditions have been shown in Fig. 2. The right side is the amplitude resolvent of the airflow output and the boundary condition of outflow is used. The air inlet has located on the left side, used the velocity inlet boundary condition. The solution domain floor of the solid wall is selected with the condition of non-slip and the top of that is also selected as symmetry [39].

Table 1 also demonstrates the amounts of the required parameters for the solution, which are used for all geometries to make the results of different domes comparable. The wind velocity of the 80 km/h was chosen based on the 20-year reports of the meteorology organizations. Based on the wind velocity of 80 km/h (10 m/s), Reynolds number (vD/ϑ) is equal to 10^7. Where, "v" is the wind velocity, "D" is the diameter of dome, and "υ" is the viscosity of the ambient air. Reynolds number is a non-dimensional number which is the ratio of inertial forces to the viscouse forces. By introducing in fact, the effect of the dimension would be eliminated automatically.

This value is much higher than 10^5 which is the transient criterion for transition of laminar flow to turbulent one for an external flow [40]. Therefore, the turbulent flow assumption is true, as it stated in Eqs. (1) to (4).

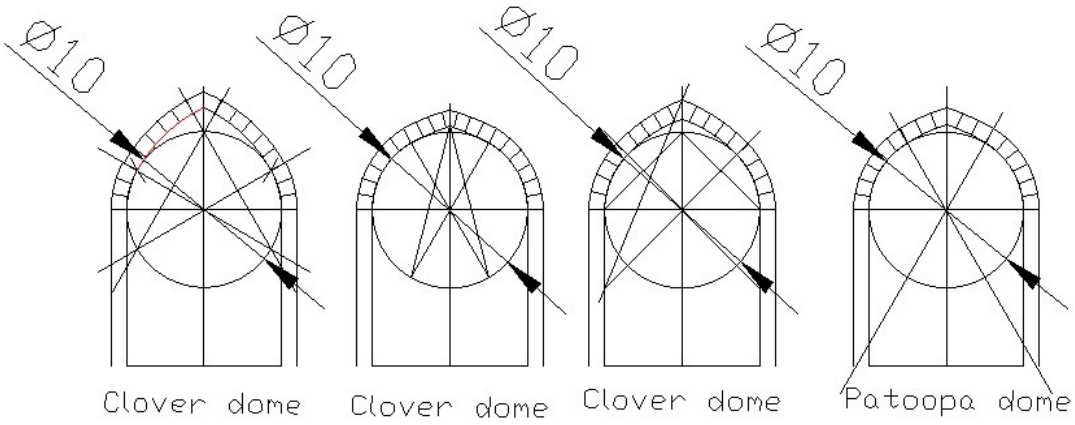

Prince Ibrahim Finn (**W1**)

Yazd Grand Mosque (**W2**)

Shahcheragh Tomb (**W3**)

Tomb of Sheikh Safi Adin Ardabili (**W4**)

Fig. 1 The dimensions, details and the real view of simulated domes.

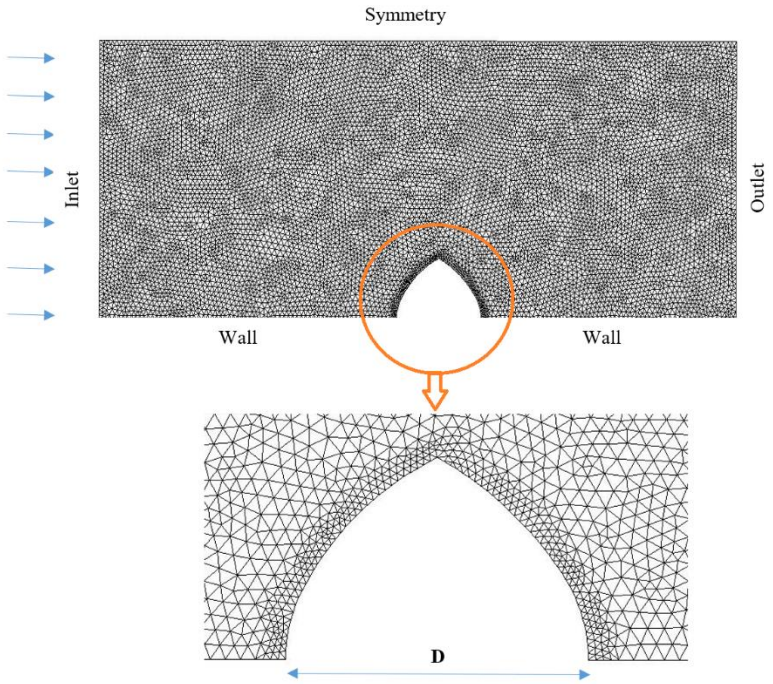

Fig. 2 A view of the solution domain grid.

Table 1. Properties and conditions of under study problem.

Re= VD/υ	Wind Velocity	Domes Diameter
0.685×10^{7}	22 m/s (80km/h)	10 m

5- Results

For the optimal design of a dome according to the construction area of the structure, the effect of the effective parameters on the strength of its outer shell should be considered. Velocity and pressure of the wind are two very influential parameters on the lifespan and durability of the structures. Wind force is an important factor in the design of structures due to its dynamic effects, and the higher the height of the structure is, the more important it becomes. In the dome examination, since the height of the structure is not very high and conversely its weight is relatively high, the dynamic effects of the wind can be considered equivalent to static loads. On one hand the wind exerts pressure on the external surface and on the other hand it creates internal pressure and suction. This internal suction and pressure on the roof are more significant as it may be combined with external pressure and suction, which might have a double effect on it.

In Fig. 3, the mesh study is discussed. W1 dome and wind speed of 80 km/h are selected for investigation. The results indicate that by changing the number of computational cells from 51261 to 101526, there is no noticeable change in the results. Therefore, to reduce the computational time, the number of meshes 51261 has been chosen for the solution. For other types of domes, this problem has also been taken into account and the optimal mesh has been used to solve it.

In view of the above, in Figs. 4 and 5, the contours of the velocity and pressure parameters on the under study domes. As it can be seen on Fig. 4, a large vortex has formed on the opposite side of the wind, affecting the area behind the dome and reducing the magnitude of the velocity. According to Fig. 5, this vortex causes negative pressure which reaches about more than 120 Pa. It can be seen on the results of Fig. 4 that the airflow is accelerated by passing over the dome and the vortex flow behind the dome brought about the highest air velocity to be formed a little higher and behind the dome. The results of Fig. 5 about the pressure contour also illustrates that the pressure on the back of the dome is negative.

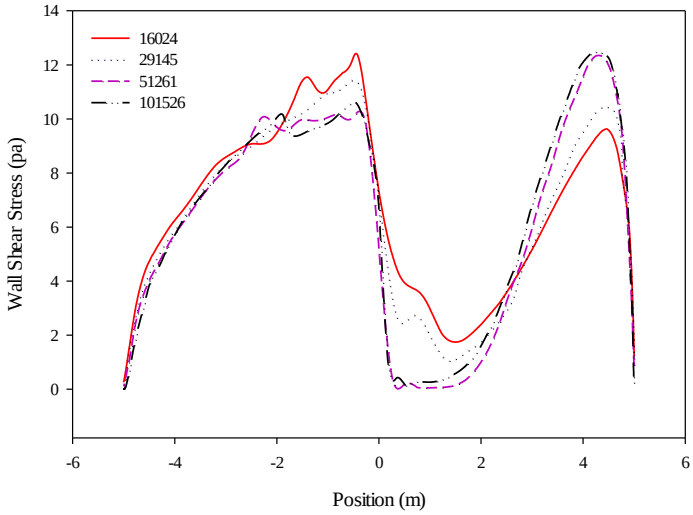

Fig. 3 The effect of grid number on the wall shear stree amount

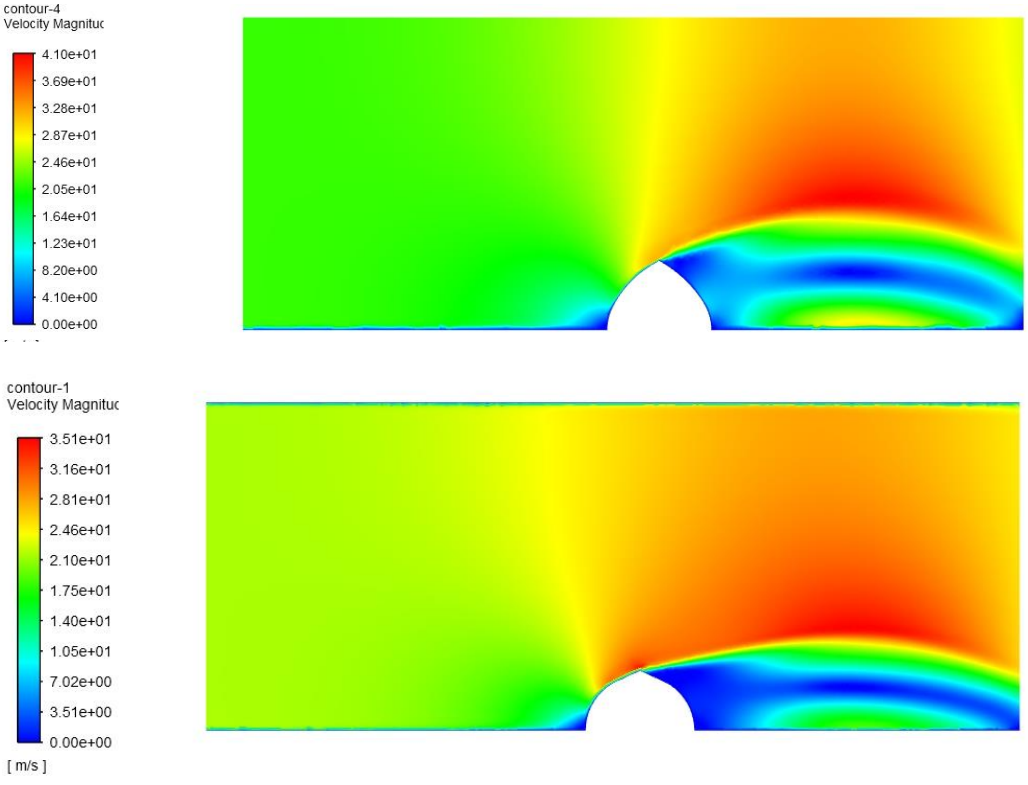

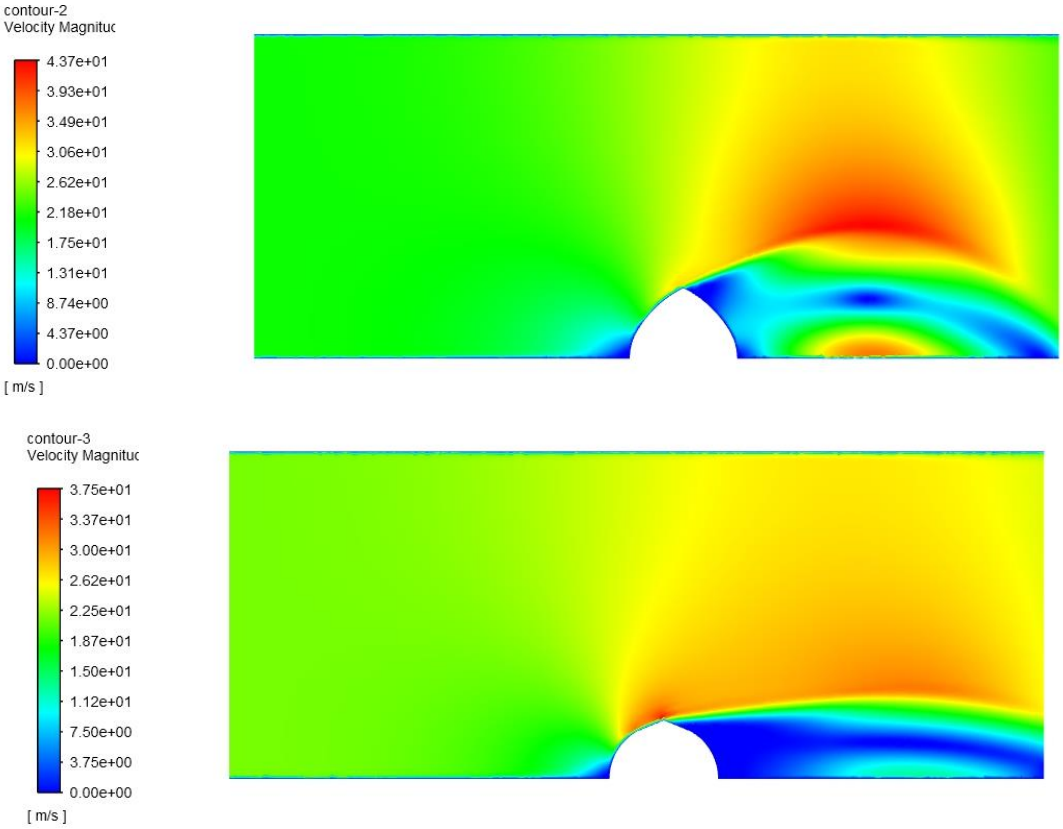

Fig. 4 Velocity contours of W1, W2, W3, and W4, respectively **(**80 km/hr of wind speed**)**.

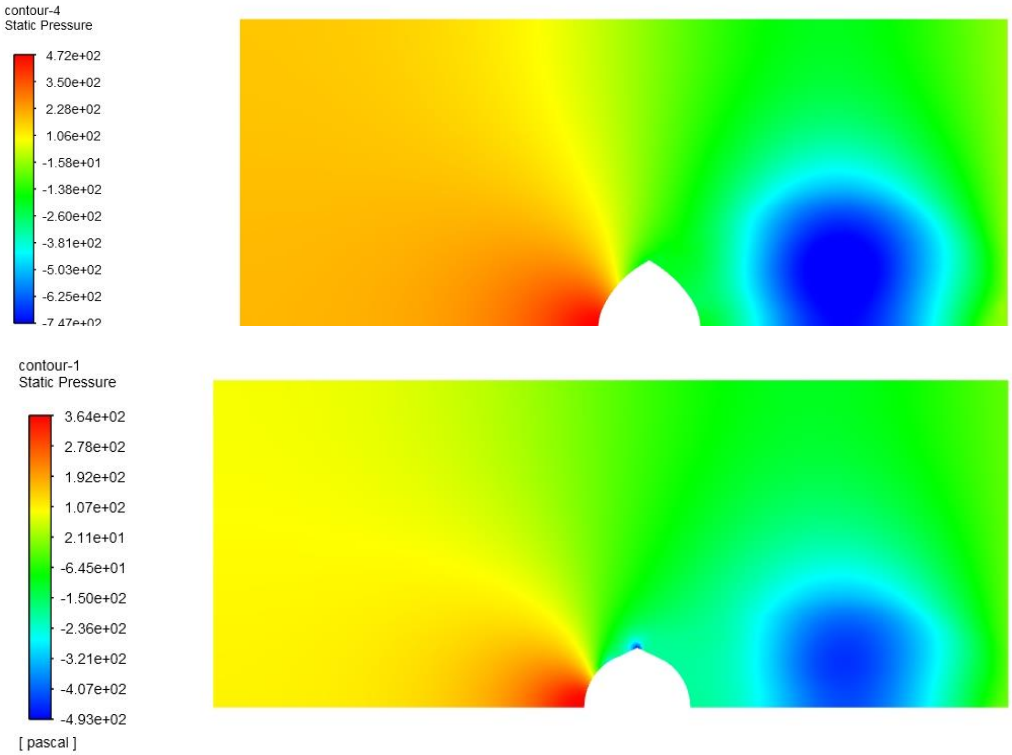

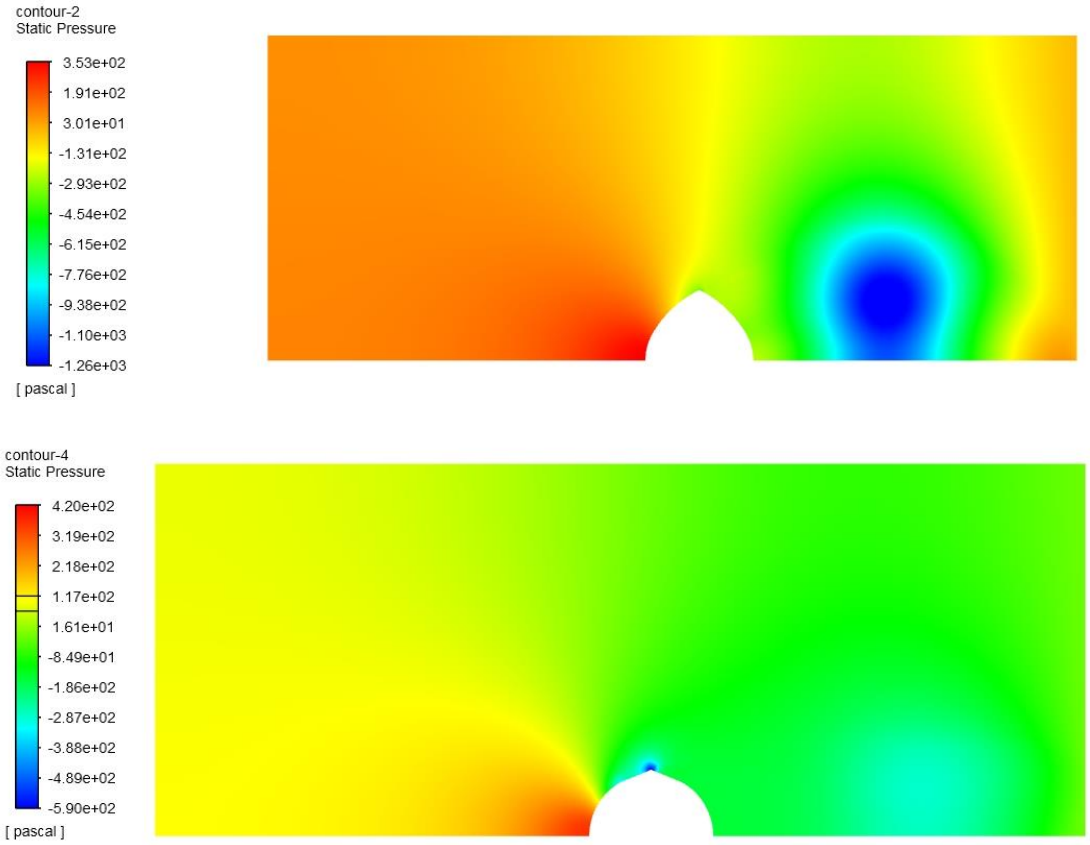

Fig. 5 Pressure contours of W1, W2, W3, and W4, respectively (80 km/hr of wind velocity).

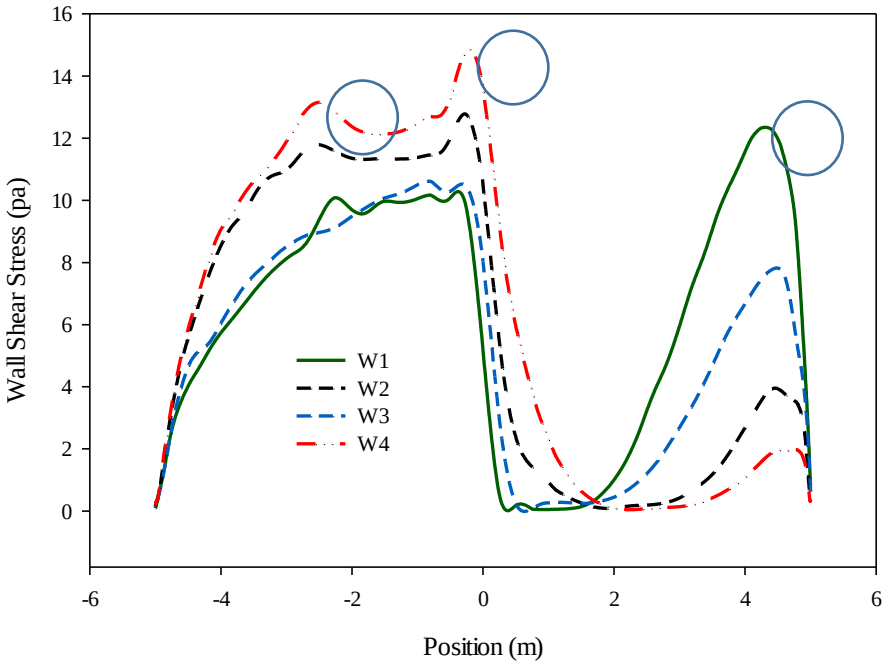

Fig. 6 The comparison of the shear stress on the crown of the dome (the vulnurable poins marked with circles).

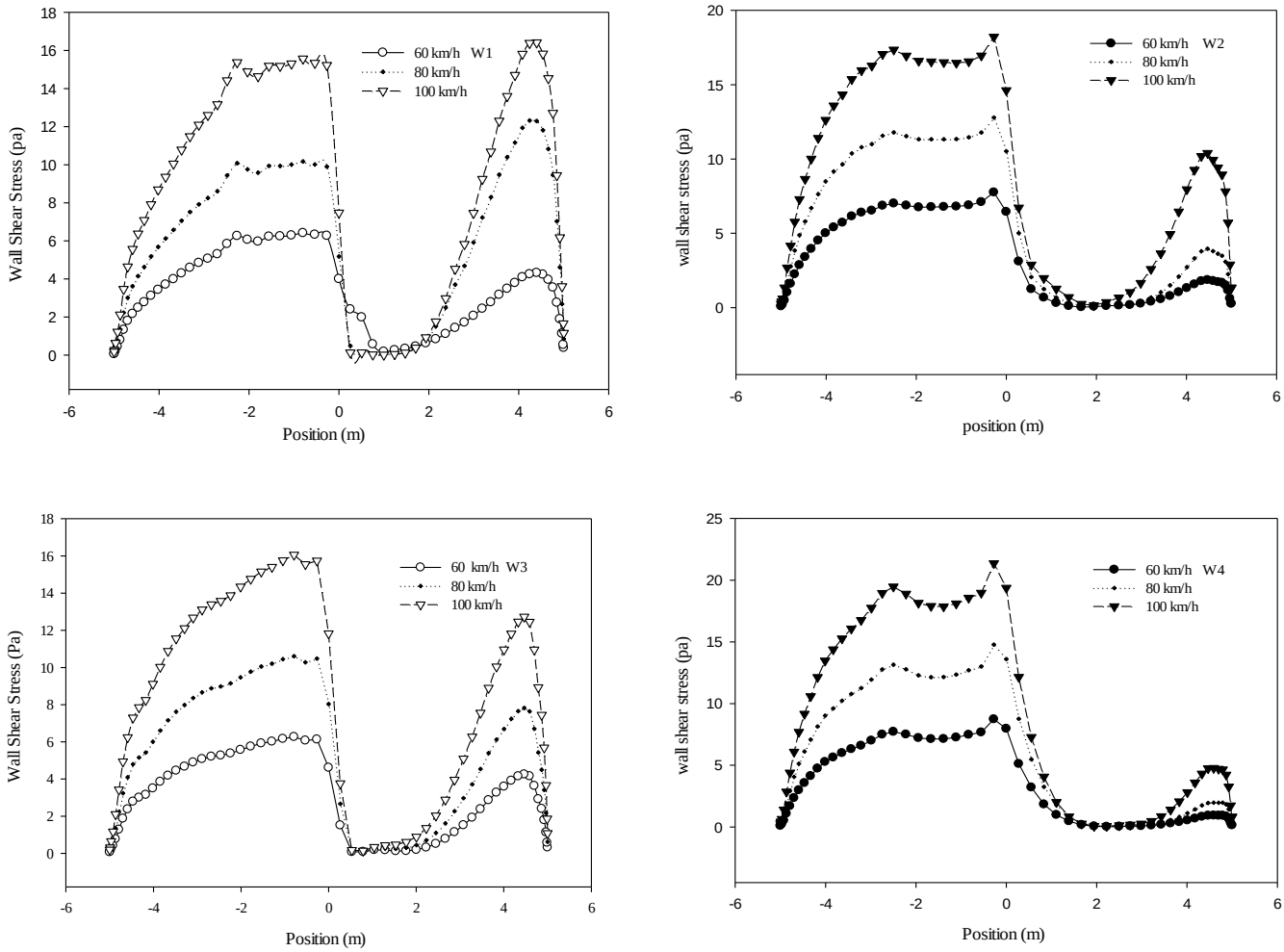

Fig. 7 The comparison of the shear stress on the crown of the dome at different wind speeds.

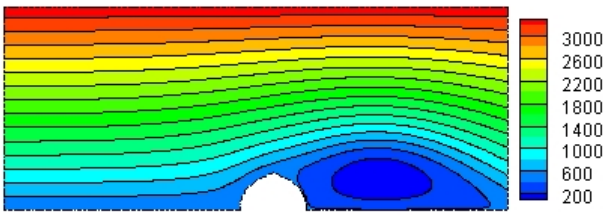

W1: Drag Force=31808.92 N

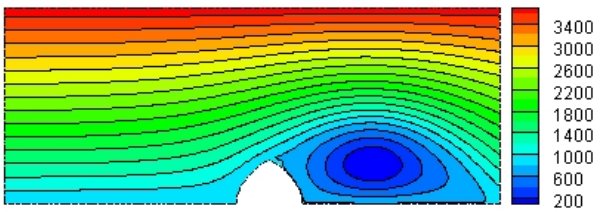

W2: Drag Force =15311.44 N

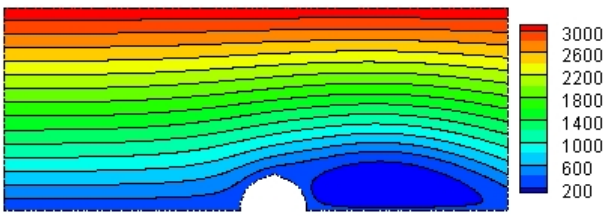

W3: Drag Force =28042.65 N

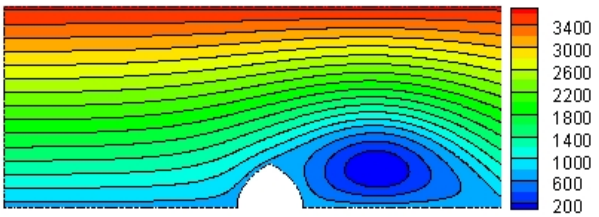

W4: Drag Force =12575.51 N

Historic structures are more eroded and damaged rather than new structures due to their long life and the long-term impact of their environmental conditions. The maintenance of these structures, which are part of the heritage and spiritual assets of countries, requires systematic strengthening and retrofitting. Therefore, by examining parameters such as shear stress on the structure, the vulnerable points of the building are identified and some solutions are provided to address them. Accordingly, the results of shear stress on the crown of the dome are shown in Fig. 6 for the four case studies and the average wind speeds of 80 km/h. Regarding to the diagram, it should be noted that the crown of the dome starts from -5 and is up to +5 (the diameter of the dome is 10 m). The results represent that for the dome W4, the highest shear stress occurs on the face against the wind with an amount of about 15 Pa and for the dome W1, it occurs on the face opposite the wind with an amount of about 12 Pa. According to the results if the shear stress on the face against the wind is high, it is less on the opposite side of the wind, and vice versa. It should be noted that the place of the most stresses on the crown of the dome is estimated to correspond to the most damages to the building. Accordingly, the volnurable points are marked on the Fig. 6.

Another important point is that the difference between shear stresses on the façade in front of the wind (maximum difference of about 30%) is less than that of against the wind (maximum difference of about 500%). In other words, the effect of different types of domes on the opposite side to the wind will present itself more. According to the results, the damage to the opposite side of the wind is very severe on the dome W1 and it is the lowest for the dome W4. Proper knowledge about the pattern of airflow and vortices around the buildings are the issues that matter in the field of wind engineering. The passing airflow through the dome creates low-pressure vortices behind it and inclines the dome to that side. If the release frequency of the vortex is equivalent to the resonance frequency of the structure, the dome will shake, that lack of attention to this problem can bring about serious damages. Fig. 7 illustrates the shear stress along with the crown of the domes in various wind speeds of 60, 80, and 100 km/h. the results show that the trends of shear stress for different wind speeds resemble those for the average speed shown in the Fig. 6. The speeds chosed one lower and another more than the average speeds. The need to check this parameter is seen more from the fact that it is mentioned that domes, despite their very high stability against symmetrical loads, are sensitive to asymmetrical loads such as wind and suffer wear and tear [41]. Fig. 7 for different domes and different wind speeds show this stress asymmetry on the crown of the dome well.

With regard to the importance of the above, Fig. 8 illustrates the contours associated with the flow for the different types of the domes, as the results indicate that the vortex formed behind the dome W1 is larger. Also, the smallest formed vortex is the dome W4 according to the results. In general, regarding the drag force exerted on the domes, it can be said that the domes W1 and W4 with the amounts of 31808 N and 12575 N have the highest and lowest drag force, respectively.

6- Conclusion

Today, due to the hardware advancements and processing power of computers, it is possible to analyze wind flow and its effects on the structure of the building with much less time and cost than wind tunnel tests. In the present work, the influence of wind on four different domes located in different climates of Iran has been investigated. For this purpose, ANSYS CFX simulation software was used for 2D solution and the parameter of shear stress exerted on the dome, pressure and velocity fields around the dome as well as flow and drag contours were examined. To be able to compare the results, dimensional analysis was used and due to the nature of the flow, the Realizable K-ε model was applied to simulate the turbulent flow around the dome. The main results are as follow:

- The maximum stress on the dome is on the facade in front of the wind, 15 Pa (the dome W4) and for the opposite side to the wind, 12 Pa (the dome W1).
- The effect of the dome type on the facade opposite to the wind is more than that of in front of the wind.
- The domes W1 and W4, with the drag forces of about 31808 N and 12575 N, have the highest and lowest drag forces on the dome, respectively.
- The vortex formed behind the dome W1 is larger and stronger.

References

[1] Feizolahbeigi, A., Lourenço, P.B., Golabchi, M., Ortega, J., Rezazadeh, M. (2020). Discussion of the role of geometry, proportion and construction techniques in the seismic behavior of 16th to 18th century bulbous discontinuous double shell domes in central Iran. Journal of Building Engineering, 33: 101575.

[2] Bakhteari, S., Attarian, K. (2020). Geometry-based modeling for characterizing design and construction of Ourchin domes. Journal of Building Engineering, 29: 101199.

[3] TehranTimes. (2020). Porticos, arches, domes and gardens, key elements of Persian architecture. https://www.tehrantimes.com/news/443707/Porticos-arches-domes-and-gardens-key-elements-of-Persian, accessed Jan. 3, 2020.

[4] Askari Chaverdi, A., Djamali, M. (2019). Sasanian Palaces of Persis According to the Absolute Chronology: Qal ‘a-ye Doxtar and Palace of Ardašīr I (Ātaškada) at Firūzābād, and the so-called Palace of Sarvestān, Iran. Archaeology Journal, 3(4): 23-32.

[5] Maroufi, H. (2020). Urban planning in ancient cities of Iran: understanding the meaning of urban form in the Sasanian city of Ardašīr-Xwarrah. Planning Perspectives, 35(6): 1055-1080.

[6] Vandaee, M., Tajbakhsh, R., Maghsoudi, R. (2013). Sassanid fire temple Discovered in Ardašīr Khore, Pars. Journal of American Science, 9: 105-114.

[7] Rezaeinia, A.A. (2018). Some Remarks on the Architectural Structure and Function of the Niasar Chahar Taq. Pazhoheshha-ye Bastan Shenasi Iran, 8(17): 141-160.

[8] Golombek, L., Wilber, D. (1988). The Timurid architecture of Iran & Turan. Princeton University Press, Princeton, New Jersey, United States.

[9] Gye, D.H. (1988). Arches and domes in Iranian Islamic Buildings: An engineer's perspective. Iran, 26(1): 129-144.

[10] Escrig, F. (1988). Towers & domes. WIT Press, Southampton SO40 7AA, UK.

[11] Grube, E.J., Dickie, J. (1995). Architecture of the Islamic world, its history & social meaning. George (EDT) Michell., William Morrow, NY.

[12] Ashkan, M., Ahmad, Y. (2010). Discontinuous double-shell domes through Islamic eras in the Middle East and central Asia: History, morphology, typologies, geometry, and construction. Nexus Network Journal, 12(2): 287-319.

[13] Ashkan, M., Ahmad, Y. (2012). Significance of conical and polyhedral domes in persia and surrounding areas: morphology, typologies and geometric characteristics. Nexus Network Journal, 14(2): 275-290.

[14] Yari, F., Silvayeh, S., Goodarzi, M., Amin, A., Hoorshenas, R. (2016). The Stability of Dome Structures in the Iranian Traditional Architecture, Case Study: Dome of Taj-al-Molk. Journal of Architectural Engineering Technology, 5(2):164.

[15] Shiri, T., Momeni, K. (2020). Investigation of the effects of sunlight on the surface of the domes of mosques in desert areas. The Journal of Geographical Research on Desert Areas, 8(1): 215-242.

[16] Behnamian, S., Behnamian, S., Fogh, F., Pashaei, F., Saran, M.M. (2020). Novelty architecture and mathematics in an Iranian mosque. Journal of Islamic Architecture, 6(1): 7-12.
[17] Danaeinia, A., Heydari Dehcheshmeh, M., Rahman, S. (2020). The Structural Solution of Light Suppling in Iranian Domeshouses. Iran University of Science & Technology, 30(1): 44-53.
[18] Faghih, A.K., Bahadori, M.N. (2009). Experimental investigation of air flow over domed roofs. Iranian Journal of Science and Technology Transaction B: Engineering, 33(3): 207–216.
[19] Cheng, C.M., Fu, C.L. (2010). Characteristic of wind loads on a hemispherical dome in smooth flow and turbulent boundary layer flow. Journal of Wind Engineering and Industrial Aerodynamics, 98(6-7): 328-344.
[20] Faghih, A.K., Bahadori, M.N. (2011). Thermal performance evaluation of domed roofs. Energy and Buildings, 43(6): 1254–1263.
[21] Abohela, I., Hamza, N., Dudek, S. (2013). Effect of roof shape on energy yield and positioning of roof mounting wind turbines. Renewable Energy, 50: 1106–1118.
[22] Sun, Y., Qiu, Y., Wu, Y. (2013). Modeling of wind pressure spectra on spherical domes. International Journal of Space Structures, 28(2): 87-99.
[23] Mahdavinejad, M., Javanroodi, K. (2014). Efficient roof shapes through wind flow and indoor temperature, case studies: Flat roofs and domed roofs. Armanshahr Architecture & Urban Development, 7(12): 55-68.
[24] Soleimani, Z., Calautit, J.K., Hughes, B.R. (2016). Computational analysis of natural ventilation flows in geodesic dome building in hot climates. Computation, 4(3): 31.
[25] Zhou, Y., Li, Y., Zhang, Y. and Yoshida, A., (2018). Characteristics of wind load on spatial structures with typical shapes due to aerodynamic geometrical parameters and terrain type. Advances in Civil Engineering, 2018: 9738038.
[26] Khosrowjerdi, S., Sarkardeh, H. and Kioumarsi, M., (2021). Effect of wind load on different heritage dome buildings. The European Physical Journal Plus, 136: 1-18.
[27] Khosrowjerdi, S. and Sarkardeh, H., (2022). Effect of wind load on combined arches in dome buildings. The European Physical Journal Plus, 137(2): 227.
[28] Nejati, A., Sadeghi, H. and Heristchian, M., (2023). Wind effect on scallop domes with negative amplitude and prominence using Experimental and Numerical Study. International Journal of Space Structures, 09560599231166897
[29] Farsani, R.Y., Mahmoudi, A., Jahangiri, M. (2020). How a conductive baffle improves melting characteristic and heat transfer in a rectangular cavity filled with gallium. Thermal Science and Engineering Progress, 16: 100453.
[30] Farsani, R.Y., Raeiszadeh, F., Jahangiri, M., Afrand, M. (2020). Melting characteristics of paraffin wax in a rectangular cavity under steady rotations. Journal of the Taiwan Institute of Chemical Engineers, 113: 135-141.
[31] Jahangiri, M., Saghafian, M., & Sadeghi, M. R. (2015). Numerical simulation of hemodynamic parameters of turbulent and pulsatile blood flow in flexible artery with single and double stenoses. Journal of Mechanical Science and Technology, 29: 3549-3560.
[32] Jahangiri, M., Saghafian, M., & Sadeghi, M. R. (2015). Effects of non-Newtonian behavior of blood on wall shear stress in an elastic vessel with simple and consecutive stenosis. Biomedical and Pharmacology Journal, 8(1): 123-131.
[33] Sharifzadeh, B., Kalbasi, R., Jahangiri, M., Toghraie, D., & Karimipour, A. (2020). Computer modeling of pulsatile blood flow in elastic artery using a software program for application in biomedical engineering. Computer methods and programs in biomedicine, 192: 105442.
[34] Jahangiri, M., Haghani, A., Ghaderi, R., & Hosseini Harat, S. M. (2018). Effect of non-Newtonian models on blood flow in artery with different consecutive stenosis. ADMT Journal: 11(1), 79-86.
[35] ANSYS, Inc. (2009). Filtered Navier-Stokes Equations, ANSYS FLUENT 12.0 Theory Guide. https://www.afs.enea.it/project/neptunius/docs/fluent/html/th/node94.htm, accessed Jan., 23, 2009.
[36] ANSYS, Inc. (2009). Standard k-ε Model, ANSYS FLUENT 12.0 Theory Guide. https://www.afs.enea.it/project/neptunius/docs/fluent/html/th/node58.htm, accessed Jan., 23, 2009.
[37] Jahangiri, M., Saghafian, M., Sadeghi, M.R., (2014). Numerical study of hemodynamic parameters in pulsatile turbulent blood flow in flexible artery with stenosis. In The 22st Annual International Conference on Mechanical Engineering-ISME2014, Shahid Chamran University, Ahvaz, Iran.
[38] Moradicheghamahi, J., Sadeghiseraji, J., Jahangiri, M. (2019). Numerical solution of the Pulsatile, non-Newtonian and turbulent blood flow in a patient specific elastic carotid artery. International Journal of Mechanical Sciences, 150: 393-403.
[39] Jahangiri, M., Saghafian, M. (2011). Numerical simulation of climb and dispersion of

pollutants in different atmospheric condition. In the 19th Annual Conference on Mechanical Engineering-ISME2011, Birjand, Iran.
[40] Pritchard, P.J., Mitchell, J.W. (2016). Fox and McDonald's Introduction to Fluid Mechanics. John Wiley & Sons. New Jersey, United States.
[41] Khosrowjerdi, S., Sarkardeh, H. (2021). Effect of arch height on wind load in shape dome structure, Amirkabir Journal of Civil Engineering, 53(2): 627-638.